Archives of Toxicology
https://doi.org/10.1007/s00204-018-2188-x

INORGANIC COMPOUNDS

Respiratory hazard of Li-ion battery components: elective toxicity of lithium cobalt oxide ($LiCoO_2$) particles in a mouse bioassay

Violaine Sironval[1] · Laurence Reylandt[2] · Perrine Chaurand[3] · Saloua Ibouraadaten[1] · Mihaly Palmai-Pallag[1] · Yousof Yakoub[1] · Bernard Ucakar[4] · Jérôme Rose[3] · Claude Poleunis[5] · Rita Vanbever[4] · Etienne Marbaix[6] · Dominique Lison[1] · Sybille van den Brule[1]

Received: 8 November 2017 / Accepted: 13 March 2018
© Springer-Verlag GmbH Germany, part of Springer Nature 2018

Abstract

Rechargeable Li-ion batteries (LIB) are increasingly produced and used worldwide. LIB electrodes are made of micrometric and low solubility particles, consisting of toxicologically relevant elements. The health hazard of these materials is not known. Here, we investigated the respiratory hazard of three leading LIB components ($LiFePO_4$ or LFP, $Li_4Ti_5O_{12}$ or LTO, and $LiCoO_2$ or LCO) and their mechanisms of action. Particles were characterized physico-chemically and elemental bioaccessibility was documented. Lung inflammation and fibrotic responses, as well as particle persistence and ion bioavailability, were assessed in mice after aspiration of LIB particles (0.5 or 2 mg); crystalline silica (2 mg) was used as reference. Acute inflammatory lung responses were recorded with the 3 LIB particles and silica, LCO being the most potent. Inflammation persisted 2 m after LFP, LCO and silica, in association with fibrosis in LCO and silica lungs. LIB particles persisted in the lungs after 2 m. Endogenous iron co-localized with cobalt in LCO lungs, indicating the formation of ferruginous bodies. Fe and Co ions were detected in the broncho-alveolar lavage fluids of LFP and LCO lungs, respectively. Hypoxia-inducible factor (HIF) -1α, a marker of fibrosis and of the biological activity of Co ions, was upregulated in LCO and silica lungs. This study identified, for the first time, the respiratory hazard of LIB particles. LCO was at least as potent as crystalline silica to induce lung inflammation and fibrosis. Iron and cobalt, but not lithium, ions appear to contribute to LFP and LCO toxicity, respectively.

Keywords Lung · Inflammation · Fibrosis · HIF-1α · Ferruginous bodies.

Background

Li-ion batteries (LIB) are used in most portable electronics such as cellular phones and laptops, and are also present in power tools, electric vehicles, etc. (Goriparti et al. 2014).

Electronic supplementary material The online version of this article (https://doi.org/10.1007/s00204-018-2188-x) contains supplementary material, which is available to authorized users.

✉ Violaine Sironval
violaine.sironval@uclouvain.be

[1] Louvain centre for Toxicology and Applied Pharmacology, Institut de Recherche Expérimentale et Clinique, Université catholique de Louvain, Avenue E. Mounier 52, bte B1.52.12, 1200 Brussels, Belgium

[2] Institute of Mechanics, Materials and Civil Engineering, Université catholique de Louvain, Place Sainte Barbe, 2, bte L5.02.02, 1348 Louvain-la-Neuve, Belgium

[3] CEREGE, Aix Marseille Université, CNRS, IRD, Collège de France, Avenue Louis Philibert, 13090 Aix en Provence, France

[4] Louvain Drug Research Institute, Université catholique de Louvain, Avenue Mounier 73, bte B1.73.12, 1200 Brussels, Belgium

[5] Institute of Condensed Matter and Nanosciences, Université catholique de Louvain, Place Louis Pasteur 1, bte L4.01.10, 1348 Louvain-la-Neuve, Belgium

[6] De Duve Institute, Université catholique de Louvain, Avenue Hippocrate 75, bte B1.75.02, 1200 Brussels, Belgium

Published online: 17 March 2018

The electrodes of conventional LIB are made of particulate materials such as lithium titanium oxide ($Li_4Ti_5O_{12}$/LTO) for the anode, and lithium cobalt oxide ($LiCoO_2$/LCO) or lithium iron phosphate ($LiFePO_4$/LFP) for the cathode (Bozich et al. 2017; Nitta et al. 2015). These materials are a source of concern because they contain (eco) toxicologically relevant elements such as lithium, cobalt, iron and nickel (Bozich et al. 2017; Kang et al. 2013). LIB particulate components are poorly water soluble and micrometric in size, suggesting that they might be respirable and biopersistent in the human respiratory tract. Currently, exposure to LIB components is potentially the most worrying for workers who produce and handle LIB particles, but future applications of LIB, such as multi-layer systems made for spray-paintable or printable batteries (Singh et al. 2012; De et al. 2017; Kim et al. 2015), could increase the potential for inhalation exposure, including for consumers. The high disposal rate of LIB and the current lack of strict regulatory policy may also lead to the dispersion of battery components in the environment and to a risk for the general population and the environment (Bozich et al. 2017). Thus, LIB particles might represent a possible inhalation risk for humans, similar to other insoluble micrometric particles or fibres inducing chronic lung inflammatory and fibrotic reactions (Leung et al. 2012; Norbet et al. 2015).

Existing knowledge on the toxicity of lithium compounds is sparse, and almost limited to systemic side effects recorded at high dose in bipolar patients treated orally with Li salts who can develop thyroid, neurological and heart toxicity (McKnight et al. 2012). LiCl inhalation induced no respiratory toxicity in rabbits (Johansson 1988) and Li combustion aerosols caused moderate lung inflammation in rats (Greenspan et al. 1986; Rebar et al. 1986). In vitro, low cytotoxicity and the secretion of the pro-inflammatory cytokine, interleukin (IL) -8, were observed in epithelial cells in response to LCO microparticles (Brog et al. 2017). In addition to Li, other LIB metallic constituents could cause toxicity. Fe and Co can cause chronic lung inflammation (Emerit et al. 2001; Lison 2015). Lung fibrosis was also observed after exposure to Co compounds (Demedts et al. 1984). Moreover, Fe and Co ions are potent inducers of oxidative stress (Jomova and Valko 2011), one of the major mechanisms incriminated in particle toxicity.

In view of the increasing production, use, disposal and almost absence of toxicological data on LIB particles, information is urgently needed to better control possible health risks. Here, we evaluated, for the first time, the lung toxicity of 3 leading LIB particles (LFP, LTO and LCO). We investigated their respective mechanisms of action to identify critical particle characteristics and key events useful for a safer-by-design and sustainable development of LIB.

Methods

Particles

LIB particles ($LiFePO_4$ or LFP, $Li_4Ti_5O_{12}$ or LTO, and $LiCoO_2$ or LCO) were obtained from MTI Corporation (Richmond, USA), lithium chloride (LiCl 730 36) from Sigma-Aldrich (Missouri, USA) and micrometric crystalline silica particles (Min-U-Sil 5, d_{50} 1.6 µm) from US Silica (Berkley Springs, USA). Before all experiments, LIB and silica particles were heated 2 h at 200 °C to remove possible endotoxin contaminants. Methods for assessing particle size, density, composition and solubilization are reported in the supplementary methods.

Animals and treatments

Female C57BL/6 mice were purchased from Janvier Labs (St Bertevin, France) or obtained from the local breeding facility (Animalerie Centrale, Université catholique de Louvain, Brussels, Belgium). Eight-week-old animals were kept with sterile rodent feed and acidified water, and housed in positive-pressure air-conditioned units (25 °C, 50% relative humidity) on a 12-h light/dark cycle. Particles and other compounds were suspended in sterile 0.9% saline solution. After anaesthesia with a mix of Nimatek, 1 mg/mouse (Eurovet, Bladel, Nederland) and Rompun, 0.2 mg/mouse (Bayer, Kiel, Germany) given intraperitoneally, 50 µl suspensions of LIB particles, silica, LiCl or NaCl (control groups) were directly administered by oro-pharyngeal aspiration. Single dose administration of particles is validated as a convenient alternative to inhalation exposure for initial hazard identification (Sabaitis et al. 1999; Driscoll et al. 2000) and induces similar lung responses as inhalation exposure (Kinaret et al. 2017; Mercer et al. 2013). Mice were sacrificed 18 h, 3 days and 2 m after administration with an intraperitoneal injection of 12 mg sodium pentobarbital (Certa, Braine-l'Alleud, Belgium).

Broncho-alveolar lavage and lung sampling

Broncho-alveolar lavage (BAL) was performed by cannulating the trachea and infusing the lungs with 1 ml NaCl 0.9%. Whole lungs were then perfused with NaCl 0.9% and excised. Left lobes were placed in 3.65% paraformaldehyde (Sigma-Aldrich, St Louis, Missouri, USA) in phosphate buffered saline (PBS) for later histological analysis, and remaining lobes in liquid nitrogen or lysis buffer for homogenization. Lungs were homogenized on ice with an Ultra-Turrax T25 (Janke and Kunkel, Brussels, Belgium) and stored at − 80 °C. Particle biopersistence was assessed

by inductively coupled plasma mass spectrometry (ICP-MS), time-of-flight secondary ion mass spectrometry (ToF-SIMS), scanning electron microscopy/energy dispersive X-ray spectrometry (SEM-EDX) and X-ray micro fluorescence (μ-XRF) (Supplementary methods). BAL was centrifuged 10 min at 4 °C (240 *g*). Cell-free supernatant (BALF) was used for biochemical measurements. After resuspension in PBS, total BAL cells were counted in Turch (crystal violet 1%, acetic acid 3%) and cytocentrifuged for differentiation by light microscopy after Diff-Quick staining (200 cells counted, Polysciences, Warrington, UK). Total proteins and lactate dehydrogenase (LDH) activity were assayed on BALF as described previously (Arras et al. 2001).

Quantification of cytokines, HIF-1α, HO-1 and lung collagen

IL-1β, IL-6, tumour necrosis factor (TNF)-α, IL-1α, transforming growth factor (TGF)-β1 and platelet-derived growth factor (PDGF)-bb were quantified by enzyme-linked immunosorbent assay (ELISA) (DuoSet ELISA, R&D Systems, Minneapolis, USA) in BALF following manufacturer's instructions. Hypoxia-inducible factor (HIF)-1α (DuoSet ELISA, R&D Systems) and heme oxygenase (HO)-1 (Immunoset, Enzo Life Sciences, Lausen, Switzerland) were assessed in supernatant (SN) of lung homogenates (centrifuged 10 min at 240*g*, 4 °C) following manufacturer's instructions. Collagen deposition was assessed by measuring the OH-proline content in lung homogenates by high-pressure liquid chromatography analysis on hydrolyzed lung homogenates as previously described (Biondi et al. 1997).

Histology

Paraffin-embedded lung sections were stained with Masson's trichrome blue (total collagen staining), Sirius Red (type I collagen staining) or Perl's Prussian blue (Fe^{3+} staining). The stained sections were scanned (Leica SCN400, Brussels, Belgium) and examined with Tissue Image Analysis 2.0 (Leica Biosystems).

Particle solubilization

To assess the bioaccessibility of elements contained in LIB particles, 10 mg LIB particles and LiCl were incubated in 10 ml artificial fluids mimicking the extracellular (pH 7.3) and the phagolysosomal (pH 4.2) compartments as previously described (Ibouraadaten et al. 2015). Particles were incubated during 30 days (at 37 °C) under gentle agitation. One ml aliquots were collected after 3, 24 h, 7 days and 30 days and centrifuged (20,000*g*, 10 min). Li, Fe, Ti and Co concentrations were determined in the SN by ICP-MS.

Statistics

Graphs and statistical analyses were performed with GraphPad Prism 5.0 and/or Microsoft excel 2013. All results are expressed as mean ± standard error on the mean (SEM). Differences between control and treated groups were evaluated using one-way analysis of variance (ANOVA) followed by a Dunnett's multiple comparison or a Newman-Keuls multiple comparison test. Statistical significance was considered at $P < 0.05$.

Results

Particle characterization

Scanning electron microscopy (SEM) (Table 1) indicated that LIB particles are micrometric in size. LFP and LTO mainly consist of aggregates, contrary to LCO. Mass median particle geometric diameter (d_{50}) measured by laser diffraction in cyclohexane was between 4 and 8 μm, with LFP = LTO < LCO. Measurements in dry state indicated strongly increased d_{50} for LFP and LTO, confirming that LFP and LTO particles form large aggregates in powder form, contrary to LCO. Particle size distributions are shown in Supplementary data Fig. S1. LCO was approximately threefold denser than LFP and LTO. The Andersen cascade impactor showed that the experimental mass median aerodynamic diameter (MMADe) was similar among the 3 particles and that all samples presented a significant respirable or fine particle fraction (FPF, aerodynamic diameter ≤ 5 μm) that can reach the deep lung when inhaled. LCO contained approximately 4 times more respirable particles than LFP or LTO. Low percentages of contaminants were detected by ICP-MS (Mn and Cu in LFP and LTO, respectively). Energy dispersive X-ray spectrometry (EDX) analysis confirmed the presence of Cu in LTO.

Bioaccessibility of metallic elements in LIB particles

To assess the release of ions from LIB particles, we analysed their bioaccessibility in artificial fluids mimicking the extracellular (pH 7.3) and the phagolysosomal (pH 4.2) compartments over a period of 30 days. Figure 1 illustrates the rate of ion release from particles, expressed as percent of initial content. As expected, LiCl was immediately and totally soluble in the tested media (Fig. 1a, e). The release of Li ions at pH 7.3 was time-dependent for LFP and LTO, whereas LCO released very low Li levels. The Fe release pattern for LFP was similar to Li at pH 4.2 (Fig. 1e, f) but not in neutral conditions, where very low Fe was released (Fig. 1a, b), suggesting that Fe ions are mainly released in the phagolysosomes. Ti was poorly bioaccessible from LTO in any

Table 1 LIB particle characterization

	LFP	LTO	LCO
Morphology[a]	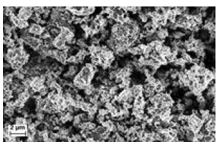	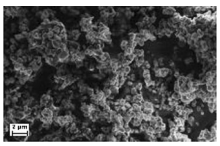	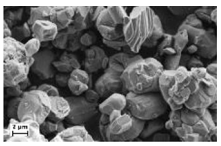
d_{50} (µm)[b]	$4.66 \pm 0.56^{*}$	$4.75 \pm 0.05^{\#}$	8.04 ± 0.17
d_{50} (µm)[c]	$28.02 \pm 8.91^{*}$	$25.23 \pm 1.15^{\#}$	6.73 ± 0.59
Density (g/cm^3)[d]	0.85	0.71	2.37
MMADe (µm)[e]	$8.20 \pm 0.57^{\$}$	13.81 ± 2.91	9.93 ± 2.27
FPF (% of total)[f]	$1.93 \pm 1.48^{*\$}$	$1.23 \pm 1.39^{\#}$	7.21 ± 1.55
C (%)[g]	Mn 0.255 ± 0.013	Cu 1.551 ± 0.124	nd
Composition[h]	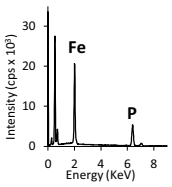	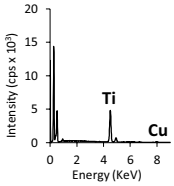	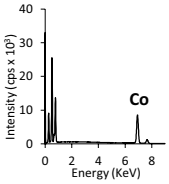

One-way ANOVA followed by a Newman-Keuls multiple comparison, $P < 0.05$, *LFP vs LCO, #LFP vs LTO, $LTO vs LCO, *nd* not detected ($n = 2$ or 3, means ± SEM)

[a]Images of LIB particles obtained by SEM

[b]Mass median particle geometric diameter (d_{50}) measured by laser diffraction in cyclohexane

[c]d_{50} measured by laser diffraction in dry state

[d]Density measured by powder tap density

[e]Experimental mass median aerodynamic diameter (MMADe) determined with an Andersen cascade impactor

[f]Fine particle fraction (FPF, ≤ 5 µm) determined with an Andersen cascade impactor

[g]Contaminant concentration (C) in mass % of LIB particles, measured by ICP-MS

[h]Particle composition obtained by EDX

condition (Fig. 1c, g), as expected from TiO_2-containing particles (Devoy et al. 2016). Finally, the patterns of Co and Li release from LCO were very similar at neutral and acidic conditions (Fig. 1a, d, e, h), LCO being preferentially solubilized at acidic pH.

LIB particles induce varying acute inflammatory responses in the lung

The lung response to LIB materials was assessed in a mouse bioassay with crystalline silica particles used as reference material. In this bioassay, inflammatory and fibrotic responses are recorded with a dose of 2-mg crystalline silica particles administered via oro-pharyngeal aspiration (Rabolli et al. 2014). LIB particles were tested at doses of 0.5 and/or 2 mg to allow benchmarking of their respiratory toxicity relative to crystalline silica particles.

After 3 d, exposure to LFP, LCO and silica resulted in acute inflammatory responses (Fig. 2). LCO induced the strongest increase in cytotoxicity (LDH activity), alveolo-capillary permeability (total proteins), inflammatory cell recruitment (macrophages and neutrophils) and secretion of pro-inflammatory mediators (IL-1β and IL-6), also compared to silica. TNF-α and IL-1α were at the control level or lower. LFP increased macrophages; TNF-α and IL-1α and LTO had no or weak effects. The expression of HO-1, a marker of oxidative stress (Nitti et al. 2017), was upregulated by all LIB particles and silica (silica < LTO < LFP < LCO).

To assess the activity of Li ions present in all LIB particles, mice were exposed to LiCl (0.85 mg) at a Li dose equimolar to 2 mg LCO which has the highest relative Li content (4.4, 6 and 7.1% Li in LFP, LTO and LCO, respectively). No effect was noted 18 h after LiCl (Supplementary data Fig. S2), suggesting that Li ions have no pro-inflammatory activity in and/or are rapidly eliminated from the lung. Differential inflammatory responses to LIB particles were also recorded after 18 h. Thus, LFP, LTO and LCO can induce acute lung inflammatory reactions of varying intensities, associated with different patterns of pro-inflammatory cytokines and oxidative stress.

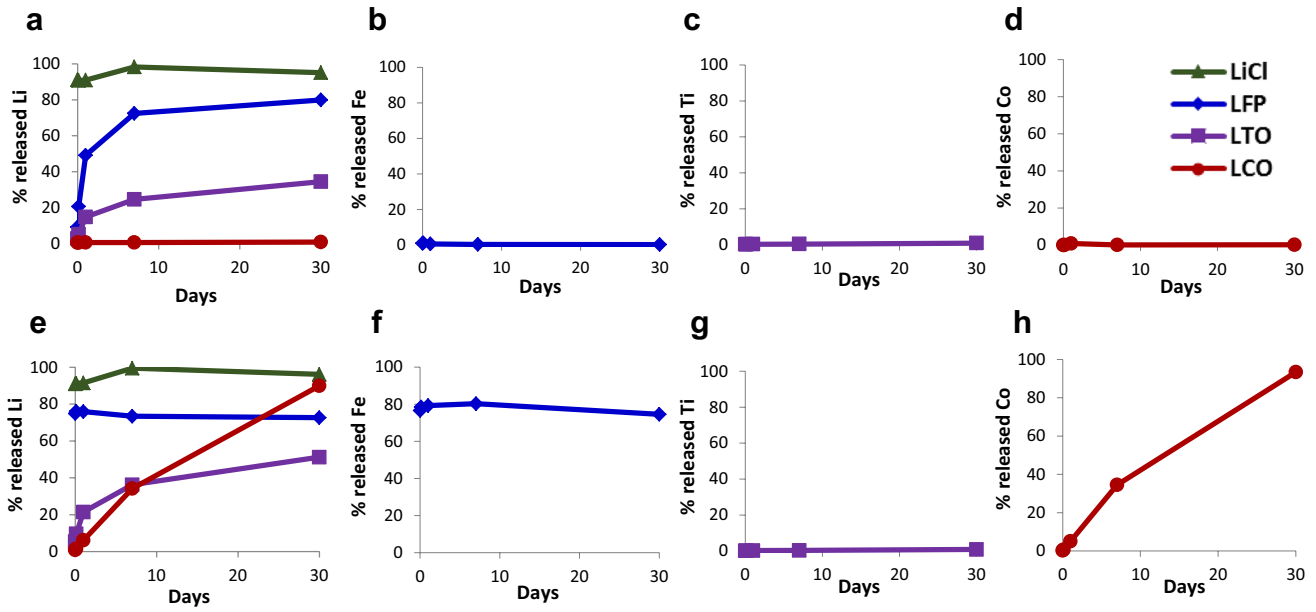

Fig. 1 Bioaccessibility of constitutive elements from LIB particles. LIB particles and LiCl were incubated in artificial fluids mimicking the extracellular (pH 7.3) (**a**–**d**) and the phagolysosomal (pH 4.2) (**e**–**h**) compartments. Particles were incubated at 37 °C under gentle agitation and released Li (**a, e**), Fe (**b, f**), Ti (**c, g**) and Co (**d, h**) concentrations were determined by ICP-MS in the SN after centrifugation of an aliquot of the suspensions after 3 h, 24 h, 7 days and 30 days

LCO induces sub-chronic inflammatory and fibrotic lung responses

Sub-chronic inflammatory and fibrotic lung responses were assessed 2 m after administration of 2 mg LIB particles, silica or 0.85 mg LiCl (Fig. 3). LDH activity and total proteins were still increased 2 m after silica and LFP. LCO induced a stronger macrophage recruitment in the alveoli compared to silica and other LIB particles while BAL neutrophils and lymphocytes were strongly increased by silica and weakly by LFP. Pro-inflammatory (IL-1β, IL-6 and IL-1α) and pro-fibrotic (TGF-β1 and PDGF-bb) cytokines in the BALF and/or lung homogenates were not increased after LIB particles (data not shown, TGF-β1 was increased by silica). LiCl and LTO had no or a weak effect on inflammatory markers. Only silica significantly increased HO-1. Accumulation of lung collagen was assessed by measuring total lung OH-proline content. OH-proline levels were only increased significantly after LCO. Lung sections stained with Sirius Red showed accumulated collagen in lungs treated with silica and LCO (Fig. 3j, m). Focal collagen accumulation, lymphoid nodules and macrophage accumulation were observed in mouse lungs 2 m after silica (Fig. 3j). Similarly, numerous lymphoid nodules around the bronchioles with focal collagen and macrophage accumulation were observed in mouse lungs after LCO (Fig. 3m). In LFP lungs, many macrophages loaded with particles (Fig. 3k) and some lymphoid nodules were observed. Compared to controls (NaCl), no overt signs of inflammation or alteration of the lung structure were observed in LTO-treated lungs (Fig. 3l). Numerous black spots of particle aggregates/agglomerates were observed by light microscopy, while very few particles were visible in LCO lungs probably because these particles do not form aggregates (Table 1). Overall, LCO induced a stronger sub-chronic inflammation than LFP and LTO, together with a fibrotic response. The fact that no reaction was detected after LiCl, together with the observation that LIB particles induced varying patterns and intensities of lung responses, further indicated that Li content is not a determinant of the lung toxicity of LIB particles. It also suggested that different mechanisms of action are involved for each LIB particle.

LIB particles persist in mouse lungs 2 m after administration

To further assess lung particle biopersistence, elements constitutive of LIB particles were first quantified by ICP-MS in lavaged lungs 18 h and 2 m after administration. After 18 h, the fraction of retained Li was higher after LCO compared to LFP and LTO (Supplementary data Fig. S3 a). Fe, Ti and Co were also detected in LFP, LTO and LCO lungs, respectively (Supplementary data Fig. S3 b–d). Retention of Li and Co was similar in LCO lungs, suggesting that intact LCO particles persisted. Ti levels were much lower than Li in LTO lungs probably because the preparation of the lung samples did not allow to completely mineralize Ti (Devoy

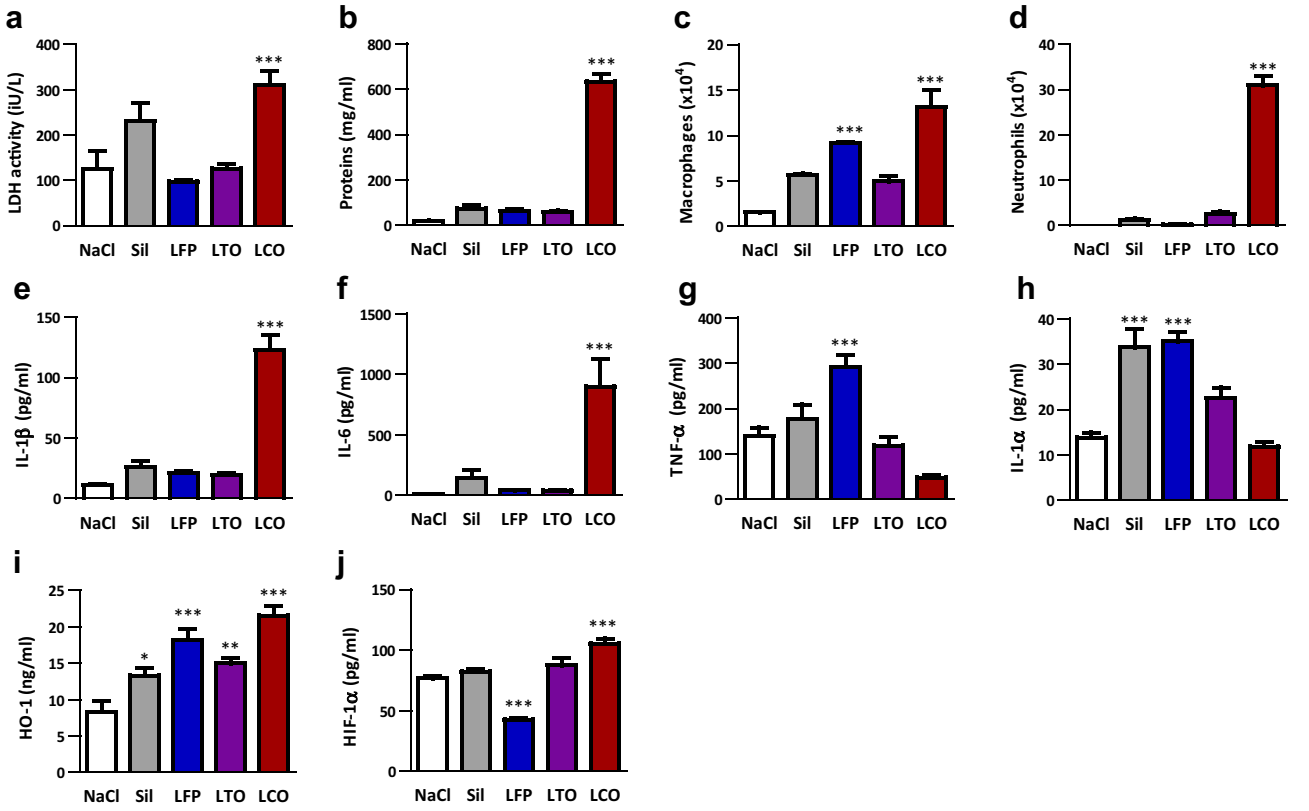

Fig. 2 LIB particles induce varying inflammatory responses after 3 days. C57BL/6 mice were exposed by oro-pharyngeal aspiration to NaCl (control), 2 mg LIB particles or crystalline silica (Sil). Inflammation was assessed in the BAL after 3 d. LDH activity (**a**) and proteins (**b**) were measured in BALF; macrophages (**c**) and neutrophils (**d**) in BAL. Inflammatory cytokines IL-1β (**e**), IL-6 (**f**), TNF-α (**g**) and IL-1α (**h**) were quantified by ELISA in the BALF; HO-1 (**i**) and HIF-1α (**j**) in lung homogenates. $*P<0.05$, $**P<0.01$ and $***P<0.001$ relative to NaCl-treated mice (one-way ANOVA followed by a Dunnett's multiple comparison, $n=5$, means ± SEM)

et al. 2016). No Li was measured in LiCl lungs, indicating that this element is quickly eliminated from the lungs. In 2-m lungs, concentrations of Li were below the limit of detection for all particles and low levels of Fe (4.5%), Ti (0.18%) and Co (0.33%) were still detected in LFP, LTO and LCO lungs, respectively (data not shown).

The persistence and localization of LIB particles, or at least their elements, were then analysed qualitatively by different techniques. A ToF-SIMS cartography on lung sections 2 m after administration revealed Li and Fe in LFP-treated lungs, Li and Ti in LTO-treated lungs and Li in LCO-treated lungs (Supplementary data Fig. S4).

Fe, Ti and Co, but not Li, could be detected on lung sections by SEM-EDX. Scanning of lung sections 2 m after administration revealed brilliant zones attributed to the presence of LIB particles (Supplementary data Fig. S5). Fe and P were detected by EDX in these zones in the lungs of LFP-treated mice, Ti in LTO-treated lungs and Co in inflammatory lung areas of LCO-treated mice. A chemical mapping of these areas was then performed (Fig. 4). In LFP-treated lungs, Fe co-localized with *P*, showing that it was still associated with the phosphate groups. Ti was detected in LTO lungs, together with Cu (data not shown) present in particles alone (Table 1). Co was detected in inflammatory/fibrotic areas of LCO lungs. A broader cartography was performed on paraffin-embedded lungs by µ-XRF. The presence of LIB particle elements in extensive areas of the lung was confirmed with a heterogeneous distribution and high-spots (Supplementary data Fig. S6). The overall results indicated that LFP, LTO and LCO persisted in the lungs.

SEM-EDX and µ-XRF analyses also showed that some Fe co-localized with Co in LCO lungs 2 m after administration (Fig. 4n and Supplementary data Fig. S6). No Fe was, however, present in original particles alone (Table 1) or after 18 h (Fig. 4s), thus suggesting a progressive deposition of endogenous Fe on the LCO particles. This was not observed with LTO and could not be assessed for LFP because of the constitutive Fe content. These observations suggested the formation of ferruginous bodies (FB) similar to those observed after asbestos exposure (Ghio et al. 2006). The distribution of Fe(III) (in blue) in lung sections exposed to LIB particles after 2 m was assessed by Perl's Prussian staining

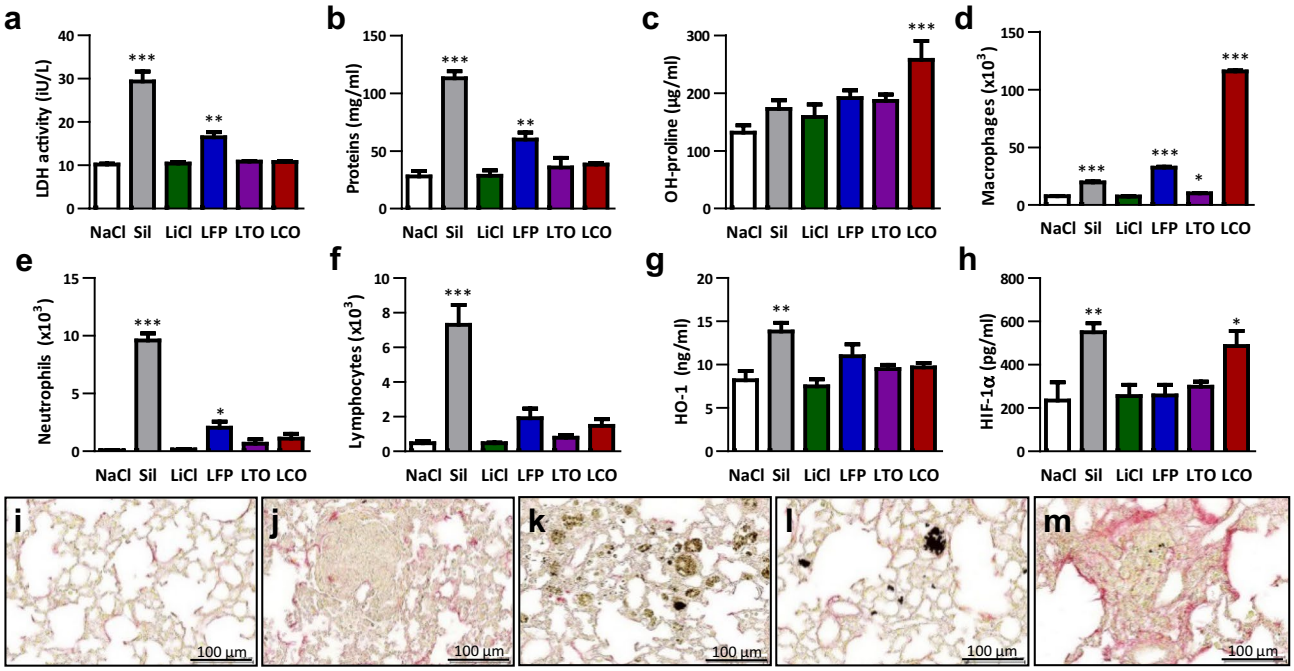

Fig. 3 Sub-chronic inflammatory and fibrotic responses to LIB particles. C57BL/6 mice were exposed by oro-pharyngeal aspiration to NaCl (control), 2 mg LIB particles or crystalline silica (Sil), and 0.85 mg LiCl. Mice were sacrificed after 2 m. Inflammation was assessed in the BAL. LDH activity (**a**) and proteins (**b**) were measured in BALF; macrophages (**d**), neutrophils (**e**) and lymphocytes (**f**) in BAL; OH-proline (**c**), HO-1 (**g**) and HIF-1α (**h**) in lung homogenates. Lung sections from mice exposed to NaCl (**i**), silica (**j**), LFP (**k**), LTO (**l**), LCO (**m**) were stained with Sirius Red. $*P<0.05$, $**P<0.01$ and $***P<0.001$ relative to NaCl-treated mice (one-way ANOVA followed by a Dunnett's multiple comparison, $n=5$, means ± SEM)

(Fig. 4e, j, o, t). Iron was detected in LFP lungs, probably due to the iron content of the particles, and in the inflammatory areas of LCO lungs. No iron staining was detected in silica (data not shown) and LTO (Fig. 4n) lungs.

In vivo bioavailability of LIB particle elements

The in vivo bioavailability of LIB metallic elements was investigated by measuring soluble elements in the BALF 18 h, 3 days and 2 m after administration. LFP released more Li in the BALF after 18 h and 3 days (Fig. 5a, e) than LTO and LCO, which was in agreement with the bioaccessibility data in artificial fluids (Fig. 2a, e). Fe, Ti and Co were also detected in the BALF after 18 h and 3 days (Fig. 5b, c, f–h) and, like Li, the % of Fe was higher in LFP BALF than Ti and Co in LTO and LCO BALF, respectively. After 2 m, low but significant levels of Li and Fe were still detected after LFP, and Co after LCO (Fig. 5i–l). These in vitro and in vivo data indicate that, in the lungs, LFP and LCO continuously release Fe and Co, respectively.

Cobalt-like responses after exposure to LCO

Because of the known pulmonary toxicity of cobalt (Simonsen et al. 2012) and the release of Co from LCO, we investigated the implication of this element in LCO lung responses by measuring HIF-1α in mouse lungs after 3 days and 2 m. HIF-1α is stabilized and accumulates in cells in response to hypoxia or Co ions (Simonsen et al. 2012). The quantification of its accumulation in lungs was used as a marker of the biological activity of Co ions. Contrary to LFP and LTO, LCO increased HIF-1α after 3 days and 2 m (Fig. 2 j and Fig. 3 h). Silica also increased HIF-1α after 2 m.

Discussion

We showed here, for the first time, that industrial LIB particles are respirable in size and can induce lung inflammatory responses with varying intensities. LTO induced a weak acute inflammation; LFP and LCO induced an acute and sub-chronic inflammation and only LCO led to fibrotic responses. The potency of LCO to induce inflammatory and fibrotic responses was at least of the same order as that of crystalline silica particles, suggesting that occupational exposure to this material should be kept below acceptable levels for crystalline silica, e.g. below 0.05 mg/m³ for the respirable fraction (SCOEL SUM/94 2003).

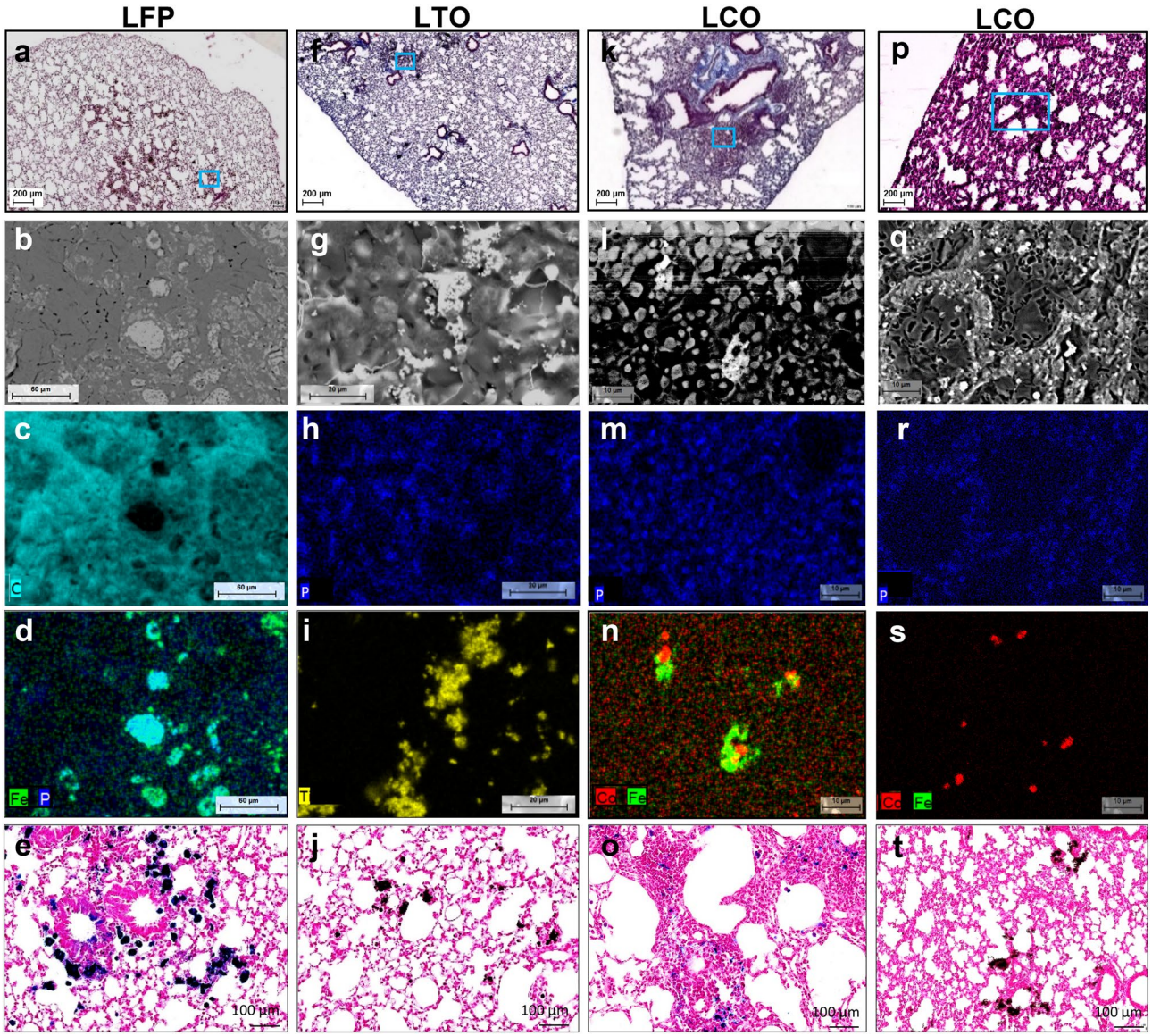

Fig. 4 Localization of LIB particle elements in lung sections by SEM-EDX after 2 m. Lung sections from mice exposed to 2 mg LFP (**a**–**e**), LTO (**f**–**j**) or LCO (**k**–**o**) were analysed after 2 m (**a**–**o**) and 18 h (**p**–**t**). Lung sections were stained with Masson's Trichrome blue (**a, f, k, p**), scanned by SEM (**b**–**d, g**–**i, l**–**n, q**–**s**) and analysed by EDX (**c, d, h, I, m, n, r, s**). Areas in blue squares (**a, f, k, p**) were zoomed and contain brilliant spots attributed to the presence of LIB particles. EDX maps show the distribution of Fe and P in LFP- (**d**), Ti in LTO- (**i**) and Fe and Co in LCO-treated lungs after 2 m (**n**) and the distribution of Co in LCO-treated lungs after 18 h (**s**). C and P distributions represent the lung matrix (**c, h, m, r**). Lung sections were stained with Perls' Prussian blue. Fe^{3+} appears in blue in LFP (**e**) and LCO (**o**) lungs after 2 m. Black spots in LTO lungs (**j**) are attributed to particles alone. After 18 h, no Fe^{3+} appears in LCO lungs (**t**). (Color figure online)

LIB particles induced an acute inflammatory response (including IL-1β, IL-6, TNF-α and IL-1α cytokines) and only LCO induced fibrosis and lymphoid nodules. Inflammatory responses play pivotal roles in pulmonary diseases induced by inhaled particles, including fibrosis (Sayan and Mossman 2016; Pardo and Selman 2002) and, therefore, might be involved in LIB toxicity. However, LCO did not exactly induce the same inflammatory pattern as silica.

Although in vitro solubilization and ToF-SIMS data support the slow release and prolonged presence of Li in the lungs exposed to LIB particles, no evidence was recorded that Li ions could be involved in the lung toxicity of LIB particles. LiCl did not induce any inflammation in vivo, even as early as 18 h after administration, as previously observed in rabbits (Johansson et al. 1988). No Li was detected in the lung at the same time point after administration of LiCl,

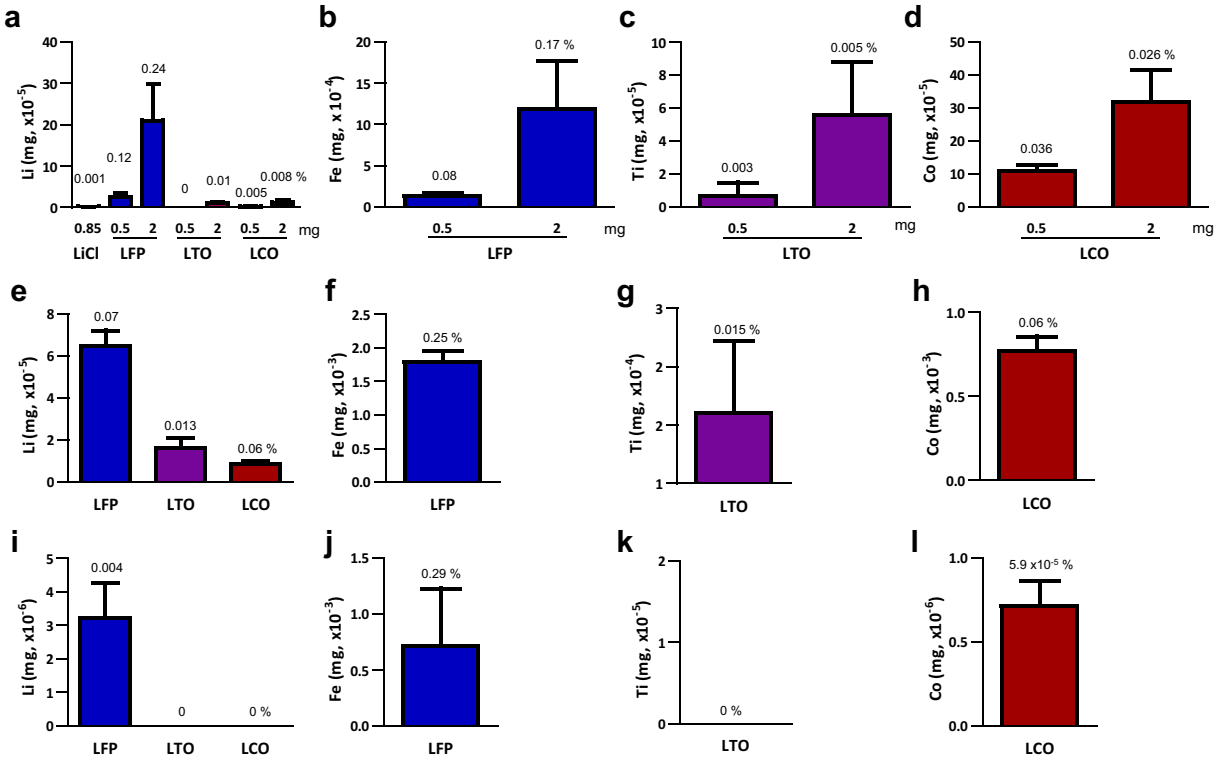

Fig. 5 Bioavailability of LIB particle elements. BALF of C57BL/6 mice exposed to NaCl, 0.85 mg LiCl, 0.5 and/or 2 mg LIB particles by oro-pharyngeal aspiration were analysed after 18 h (**a**–**d**), 3 days (**e**–**h**) or 2 m (**i**–**l**). Li (**a, e, i**), Fe from LFP (**b, f, j**), Ti from LTO (**c, g, k**) and Co from LCO (**d, h, l**) particles were measured by ICP-MS. Percentages were calculated on the basis of initial Li, Fe, Ti, Co particle content after subtraction of levels measured in NaCl-treated lungs ($n = 5$, means ± SEM)

suggesting that Li ions are rapidly washed out from the lung. Finally, the varying responses to the 3 Li-containing particles (LFP, LTO and LCO) in the mouse bioassay do not argue in favour of a critical role of Li in LIB lung toxicity.

LTO particles induced an acute inflammation and persisted in mouse lungs 2 m after administration but no inflammation or fibrosis was detected at this time point. The low toxicity of LTO can be attributed to its TiO_2 content (Han et al. 2013) which is considered a low toxicity material. Inhalation of TiO_2 appears to induce low acute inflammation and no fibrosis (Shi et al. 2013; Yoshiura et al. 2015), which is in agreement with our observations.

Inflammatory responses and persisting particles in the lung interstitium were observed 2 m after administration of LFP. Inhalation of iron compounds can lead to siderosis, a benign pneumoconiosis with little or no fibrosis (Nemery 1990). However, free Fe in excess catalyses free radical formation, which induces cytotoxicity and oxidative stress, leading to cellular damages, carcinogenicity and mutagenicity (Emerit et al. 2001) as also reported for particles such as asbestos (Gazzano et al. 2007). Our data showed that LFP can release Fe ions in vivo and in vitro and increase the expression of HO-1. The transient pulmonary inflammation induced by LFP can thus be explained by its Fe content.

LCO particles appeared more potent than LFP and LTO. Administration of LCO induced acute and sub-chronic lung inflammation, and fibrosis in mice. In addition to pro-inflammatory mediators and structural modifications observed in the lungs exposed to LCO particles, these effects were accompanied by the persistence of their constitutive elements (Li and Co), the presence of FB, the increase of HO-1 and accumulation of HIF-1α. Pulmonary diseases (cancer, asthma and fibrosing alveolitis) have previously been reported in workers exposed to cobalt (Demedts et al. 1984; Jomova and Valko 2011). A well-documented example of fibrosis caused by Co is due to the association of tungsten carbide with Co metal powder (Lasfargues et al. 1992). Cobalt compounds can also induce cytotoxicity, apoptosis, inflammatory responses and genotoxicity in vitro (Simonsen et al. 2012). Some of the effects of cobalt are related to its high affinity for sulfhydryl groups leading to enzyme inactivation, to its antagonism for Ca^{2+} channel modifying cell signalling, to its production of reactive oxygen species leading to an oxidative stress, and finally to its ability to stabilize HIF-1α (Simonsen et al. 2012). The two latter mechanisms were identified with LCO, suggesting that Co plays an important role in LCO lung toxicity. HO-1, a robust oxidative stress marker, was increased 3 days after LCO,

suggesting that LCO can induce an oxidative stress in mouse lungs. The fact that only LCO induced the accumulation of HIF-1α contrary to LFP and LTO highlights the importance of cobalt in LIB particle toxicity.

Iron co-localized with Co in mouse lungs 2 m after administration of LCO, suggesting the formation of FB. FB are particles or fibres coated with proteins and iron from the endogenous milieu (Ghio et al. 2004) and were detected in lungs exposed to asbestos fibres (Pascolo et al. 2016). LCO-induced lung inflammation could cause the disruption of iron lung homeostasis as observed during infection and inflammation (Fahmy and Young 1993; Ganz and Nemeth 2015) and lead to the local increase of particle-associated iron. FB are thought to participate to lung toxicity, including fibrosis, by catalysing Fenton reactions and free radical generation (Ghio et al. 2004, 2006; Fubini 1997). This phenomenon could thus contribute, together with Co ions, to the elective lung toxicity of LCO. The oxidative potential of LCO particles, as well as the contribution of FB in this process, must be the subject of additional investigations.

As previously mentioned, only LCO induced HIF-1α accumulation reflecting the intensity of its pulmonary toxicity as compared to other LIB particles. HIF-1α is a pro-inflammatory and carcinogenic transcriptional factor continuously expressed in all cells. Under normoxic conditions, HIF-1α is directly degraded by the ubiquitin–proteasome pathway, via a prolyl hydroxylase (PH). However, under hypoxic conditions, HIF-1α is stabilized and accumulates in the cell (Weidemann and Johnson 2008; Jochmanova et al. 2013). Co(II) ions are also able to stabilize HIF-1α by blocking the iron-binding site of PH and by direct binding to HIF-1α preventing its degradation (Epstein et al. 2001; Yuan et al. 2003). HIF-1α plays many roles in inflammation and induces the secretion of inflammatory mediators (Jochmanova et al. 2013). Its expression is also increased in animal models of bleomycin- and paraquat-induced lung fibrosis and in idiopathic lung fibrosis patients (Zhu et al. 2016; Ruthenborg et al. 2014). In addition, we have shown here that HIF-1α is accumulated during the fibrotic phase of the silica model, reinforcing the association between this mediator and fibrosis. HIF-1α plays a role in fibrosis by promoting myofibroblast differentiation and epithelial-mesenchymal transition via the TGF-β pathway (Zhou et al. 2009; Zhu et al. 2016; Zhao et al. 2017). HIF-1α thus appears as a very useful biomarker of LCO particle toxicity as it not only allows tracing the bioavailability of Co ions, but could also contribute mechanistically to the inflammatory and fibrotic responses induced by LCO. Interestingly, although some studies showed that the HO-1 response can increase HIF-1α expression (Jochmanova et al. 2013; Nitti et al. 2017), LFP upregulated HO-1 but did not increase HIF-1α.

In addition to the potential mechanisms identified above for LCO lung toxicity, it should be noted that LCO contains the highest FPF and forms less aggregates than LFP and LTO, as indicated by the SEM images and the laser diffraction analysis in dry state (Table 1). Furthermore, many aggregates were observed in LFP and LTO lung sections 2 m after exposure contrary to LCO (Fig. 3k–m). Given that particle size and formation of aggregates can modulate their reactivity toward cells and tissues (Fubini 1997), it is very likely that these parameters also contribute to the elective toxicity of LCO by a more efficient dispersion and bioavailability of LCO particles/elements in the lung.

Thus, LCO was able to induce early oxidative stress responses, secretion of inflammatory mediators and HIF-1α accumulation. These responses are, at least partially, attributed to the Co content of LCO. Although it appears premature to conclude on the exact sequence of events, the formation of FB appears to be a consequence of the early inflammatory responses to LCO. Taken together, particle size distribution, Co ions/HIF-1α and ferruginous bodies/oxidative stress could represent the pathogenic cocktail responsible of the elective lung toxicity of LCO particles in the present study.

We conclude that LIB particles represent a respiratory hazard. Exposure to LIB particles should, therefore, be strictly controlled in occupational settings, and the life cycle of these components should be adequately monitored to avoid environmental pollution and indirect exposure of consumers and the general population.

Acknowledgements We warmly thank Marc de Bournonville (Institut de Recherche Expérimentale et Clinique, Université catholique de Louvain) for his help with histological staining and Gladys Deumer (Cliniques Universitaires St Luc) for her help with ICP-MS analysis. The "Programme d'excellence BATWAL 1318146 from the SPW DG06 (Belgium)" supported the research project and financed Sybille van den Brule. Violaine Sironval is financed by a grant from the "Fonds pour la Formation à la Recherche dans l'Industrie et dans l'Agriculture (FRIA)".

Compliance with ethical standards

Conflict of interest The authors declare that they have no conflict of interest.

Ethical approval All applicable international, national institutional guidelines for the care and use of animals were followed. All procedures performed in studies involving animals were in accordance with the ethical standards of the institution (Université catholique de Louvain, Comité d'Ethique pour l'Expérimentation Animale, Secteur des Sciences de la Santé, Brussels, Belgium (No LA1230312)) or practice at with the studies were conducted.

Informed consent This article does not contain any studies with human participants performed by any of the authors.

References

Arras M, Huaux F, Vink A, Delos M, Coutelier JP, Many MC, Barbarin V, Renauld JC, Lison D (2001) Interleukin-9 reduces lung fibrosis and type 2 immune polarization induced by silica particles in a murine model. Am J Respir Cell Mol Biol 24:368–375. https://doi.org/10.1165/ajrcmb.24.4.4249

Biondi PA, Chiesa LM, Storelli MR, Renon P (1997) A new procedure for the specific high-performance liquid chromatographic determination of hydroxyproline. J Chromatogr Sci 35:509–512

Bozich J, Hang M, Hamers R, Klaper R (2017) Core chemistry influences the toxicity of multicomponent metal oxide nanomaterials, lithium nickel manganese cobalt oxide, and lithium cobalt oxide to Daphnia magna. Environ Toxicol Chem 9999:1–10. https://doi.org/10.1002/etc.3791

Brog JP, Crochet A, Seydoux J, Clift MJD, Baichette B, Maharajan S, Barosova H, Brodard P, Spodaryk M, Zuttel A, Rothen-Rutishauser B, Kwon NH, Fromm KM (2017) Characteristics and properties of nano-LiCoO2 synthesized by pre-organized single source precursors: Li-ion diffusivity, electrochemistry and biological assessment. J Nanobiotechnol 15:58. https://doi.org/10.1186/s12951-017-0292-3

De B, Yadav A, Khan S, Kar KK (2017) A facile methodology for the development of a printable and flexible all-solid-state rechargeable battery. ACS Appl Mater Interfaces 9:19870–19880. https://doi.org/10.1021/acsami.7b04112

Demedts M, Gheysens B, Nagels J, Verbeken E, Lauweryns J, van den Eeckhout A, Lahaye D, Gyselen A (1984) Cobalt lung in diamond polishers. Am Rev Respir Dis 130:130–135. https://doi.org/10.1164/arrd.1984.130.1.130

Devoy J, Brun E, Cosnefroy A, Disdier C, Melczer M, Antoine G, Chalansonnet M, Mabonzo A (2016) Mineralization of TiO_2 nanoparticles for the determination of titanium in rat tissues. J Anal Chem 71:418–425

Driscoll KE, Costa DL, Hatch G, Henderson R, Oberdorster G, Salem H, Schlesinger RB (2000) Intratracheal instillation as an exposure technique for the evaluation of respiratory tract toxicity: uses and limitations. Toxicol Sci 55:24–35

Emerit J, Beaumont C, Trivin F (2001) Iron metabolism, free radicals, and oxidative injury. Biomed Pharmacother 55:333–339

Epstein AC, Gleadle JM, McNeill LA, Hewitson KS, O'Rourke J, Mole DR, Mukherji M, Metzen E, Wilson MI, Dhanda A, Tian YM, Masson N, Hamilton DL, Jaakkola P, Barstead R, Hodgkin J, Maxwell PH, Pugh CW, Schofield CJ, Ratcliffe PJ (2001) C. elegans EGL-9 and mammalian homologs define a family of dioxygenases that regulate HIF by prolyl hydroxylation. Cell 107:43–54

Fahmy M, Young SP (1993) Modulation of iron metabolism in monocyte cell line U937 by inflammatory cytokines: changes in transferrin uptake, iron handling and ferritin mRNA. Biochem J 296(Pt 1):175–181

Fubini B (1997) Surface reactivity in the pathogenic response to particulates. Environ Health Perspect 105 (5):1013–1020

Ganz T, Nemeth E (2015) Iron homeostasis in host defence and inflammation. Nat Rev Immunol 15:500–510. https://doi.org/10.1038/nri3863

Gazzano E, Turci F, Foresti E, Putzu MG, Aldieri E, Silvagno F, Lesci IG, Tomatis M, Riganti C, Romano C, Fubini B, Roveri N, Ghigo D (2007) Iron-loaded synthetic chrysotile: a new model solid for studying the role of iron in asbestos toxicity. Chem Res Toxicol 20:380–387. https://doi.org/10.1021/tx600354f

Ghio AJ, Churg A, Roggli VL (2004) Ferruginous bodies: implications in the mechanism of fiber and particle toxicity. Toxicol Pathol 32:643–649. https://doi.org/10.1080/01926230490885733

Ghio AJ, Funkhouser W, Pugh CB, Winters S, Stonehuerner JG, Mahar AM, Roggli VL (2006) Pulmonary fibrosis and ferruginous bodies associated with exposure to synthetic fibers. Toxicol Pathol 34:723–729. https://doi.org/10.1080/01926230600932448

Goriparti S, Miele E, De Angelis F, Di Fabrizio E, Zaccaria R, Capiglia C (2014) Review on recent progress of nanostructured anode materials for Li-ion batteries. J Power Sources 257:421–443

Greenspan BJ, Allen MD, Rebar AH (1986) Inhalation toxicity of lithium combustion aerosols in rats. J Toxicol Environ Health 18:627–637. https://doi.org/10.1080/15287398609530899

Han SW, Ryu JH, Jeong J, Yoon DH (2013) Solid-state synthesis of Li4Ti5O12 for high power lithium ion battery applications. J Alloys comp 570:144–149

Ibouraadaten S, van den Brule S, Lison D (2015) Does carbonation of steel slag particles reduce their toxicity? An in vitro approach. Toxicol In Vitro 29:722–726. https://doi.org/10.1016/j.tiv.2015.02.013

Jochmanova I, Yang C, Zhuang Z, Pacak K (2013) Hypoxia-inducible factor signaling in pheochromocytoma: turning the rudder in the right direction. J Natl Cancer Inst 105:1270–1283. https://doi.org/10.1093/jnci/djt201

Johansson A, Camner P, Curstedt T, Jarstrand C, Robertson B, Urban T (1988) Rabbit lung after inhalation of lithium chloride. J Appl Toxicol 8:373–375

Jomova K, Valko M (2011) Advances in metal-induced oxidative stress and human disease. Toxicology 283:65–87. https://doi.org/10.1016/j.tox.2011.03.001

Kang DH, Chen M, Ogunseitan OA (2013) Potential environmental and human health impacts of rechargeable lithium batteries in electronic waste. Environ Sci Technol 47:5495–5503. https://doi.org/10.1021/es400614y

Kim SH, Choi KH, Cho SJ, Choi S, Park S, Lee SY (2015) Printable solid-state lithium-ion batteries: a new route toward shape-conformable power sources with aesthetic versatility for flexible electronics. Nano Lett 15:5168–5177. https://doi.org/10.1021/acs.nanolett.5b01394

Kinaret P, Ilves M, Fortino V, Rydman E, Karisola P, Lahde A, Koivisto J, Jokiniemi J, Wolff H, Savolainen K, Greco D, Alenius H (2017) Inhalation and oropharyngeal aspiration exposure to rod-like carbon nanotubes induce similar airway inflammation and biological responses in mouse lungs. ACS Nano 11:291–303. https://doi.org/10.1021/acsnano.6b05652

Lasfargues G, Lison D, Maldague P, Lauwerys R (1992) Comparative study of the acute lung toxicity of pure cobalt powder and cobalt-tungsten carbide mixture in rat. Toxicol Appl Pharmacol 112:41–50

Leung CC, Yu IT, Chen W (2012) Silicosis Lancet 379:2008–2018. https://doi.org/10.1016/S0140-6736(12)60235-9

Lison D (2015) Cobalt. In: Nordberg GF, Fowler BA, Nordberg M (eds) Handbook on the toxicology of metals, 4th edn. Elsevier, Paris, pp 743–763

McKnight RF, Adida M, Budge K, Stockton S, Goodwin GM, Geddes JR (2012) Lithium toxicity profile: a systematic review and meta-analysis. Lancet 379:721–728. https://doi.org/10.1016/S0140-6736(11)61516-X

Mercer RR, Scabilloni JF, Hubbs AF, Battelli LA, McKinney W, Friend S, Wolfarth MG, Andrew M, Castranova V, Porter DW (2013) Distribution and fibrotic response following inhalation exposure to multi-walled carbon nanotubes. Part Fibre Toxicol 10:33. https://doi.org/10.1186/1743-8977-10-33

Nemery B (1990) Metal toxicity and the respiratory tract. Eur Respir J 3:202–219

Nitta N, Wu F, Lee JT, Yushin G (2015) Li-ion battery materials: present and future. Mater Today 18:252–264

Nitti M, Piras S, Marinari UM, Moretta L, Pronzato MA, Furfaro AL (2017) HO-1 induction in cancer progression: a matter of cell adaptation. Antioxidants (Basel) 6:29. https://doi.org/10.3390/antiox6020029

Norbet C, Joseph A, Rossi SS, Bhalla S, Gutierrez FR (2015) Asbestos-related lung disease: a pictorial review. Curr Probl Diagn Radiol 44:371–382. https://doi.org/10.1067/j.cpradiol.2014.10.002

Pardo A, Selman M (2002) Molecular mechanisms of pulmonary fibrosis. Front Biosci 7:d1743-d1761

Pascolo L, Zabucchi G, Gianoncelli A, Kourousias G, Trevisan E, Pascotto E, Casarsa C, Ryan C, Lucattelli M, Lungarella G, Cavarra E, Bartalesi B, Zweyer M, Cammisuli F, Melato M, Borelli V (2016) Synchrotron X-ray microscopy reveals early calcium and iron interaction with crocidolite fibers in the lung of exposed mice. Toxicol Lett 241:111–120. https://doi.org/10.1016/j.toxlet.2015.11.016

Rabolli V, Badissi AA, Devosse R, Uwambayinema F, Yakoub Y, Palmai-Pallag M, Lebrun A, De G, Couillin V, Ryffel I, Marbaix B, Lison E, Huaux D F (2014) The alarmin IL-1alpha is a master cytokine in acute lung inflammation induced by silica micro- and nanoparticles. Part Fibre Toxicol 11:69. https://doi.org/10.1186/s12989-014-0069-x

Rebar AH, Greenspan BJ, Allen MD (1986) Acute inhalation toxicopathology of lithium combustion aerosols in rats. Fundam Appl Toxicol 7:58–67

Ruthenborg RJ, Ban JJ, Wazir A, Takeda N, Kim JW (2014) Regulation of wound healing and fibrosis by hypoxia and hypoxia-inducible factor-1. Mol Cells 37:637–643. https://doi.org/10.14348/molcells.2014.0150

Sabaitis CP, Leong BK, Rop DA, Aaron CS (1999) Validation of intratracheal instillation as an alternative for aerosol inhalation toxicity testing. J Appl Toxicol 19:133–140

Sayan M, Mossman BT (2016) The NLRP3 inflammasome in pathogenic particle and fibre-associated lung inflammation and diseases. Part Fibre Toxicol 13:51. https://doi.org/10.1186/s12989-016-0162-4

SCOEL SUM/94 (2003) Recommendation from the Scientific Committee on Occupational Exposure Limits for Silica, Crystalline (respirable dust)

Shi H, Magaye R, Castranova V, Zhao J (2013) Titanium dioxide nanoparticles: a review of current toxicological data. Part Fibre Toxicol 10:15. https://doi.org/10.1186/1743-8977-10-15

Simonsen LO, Harbak H, Bennekou P (2012) Cobalt metabolism and toxicology—a brief update. Sci Total Environ 432:210–215. https://doi.org/10.1016/j.scitotenv.2012.06.009

Singh N, Galande C, Miranda A, Mathkar A, Gao W, Reddy AL, Vlad A, Ajayan PM (2012) Paintable battery. Sci Rep 2:481. https://doi.org/10.1038/srep00481

Weidemann A, Johnson RS (2008) Biology of HIF-1alpha. Cell Death Differ 15:621–627. https://doi.org/10.1038/cdd.2008.12

Yoshiura Y, Izumi H, Oyabu T, Hashiba M, Kambara T, Mizuguchi Y, Lee BW, Okada T, Tomonaga T, Myojo T, Yamamoto K, Kitajima S, Horie M, Kuroda E, Morimoto Y (2015) Pulmonary toxicity of well-dispersed titanium dioxide nanoparticles following intratracheal instillation. J Nanopart Res 17:241. https://doi.org/10.1007/s11051-015-3054-x

Yuan Y, Hilliard G, Ferguson T, Millhorn DE (2003) Cobalt inhibits the interaction between hypoxia-inducible factor-alpha and von Hippel-Lindau protein by direct binding to hypoxia-inducible factor-alpha. J Biol Chem 278:15911–15916. https://doi.org/10.1074/jbc.M300463200

Zhao B, Guan H, Liu JQ, Zheng Z, Zhou Q, Zhang J, Su LL, Hu DH (2017) Hypoxia drives the transition of human dermal fibroblasts to a myofibroblast-like phenotype via the TGF-beta1/Smad3 pathway. Int J Mol Med 39:153–159. https://doi.org/10.3892/ijmm.2016.2816

Zhou G, Dada LA, Wu M, Kelly A, Trejo H, Zhou Q, Varga J, Sznajder JI (2009) Hypoxia-induced alveolar epithelial-mesenchymal transition requires mitochondrial ROS and hypoxia-inducible factor 1. Am J Physiol Lung Cell Mol Physiol 297:L1120-L1130. https://doi.org/10.1152/ajplung.00007.2009

Zhu Y, Tan J, Xie H, Wang J, Meng X, Wang R (2016) HIF-1alpha regulates EMT via the Snail and beta-catenin pathways in paraquat poisoning-induced early pulmonary fibrosis. J Cell Mol Med 20:688–697. https://doi.org/10.1111/jcmm.12769